Chemical Science

ROYAL SOCIETY OF CHEMISTRY

EDGE ARTICLE

View Article Online
View Journal | View Issue

Cite this: *Chem. Sci.*, 2025, **16**, 23246

All publication charges for this article have been paid for by the Royal Society of Chemistry

Photoredox catalysed reductive cleavage of dibenzothiophene dioxides enabled by a temperature-controlled photoreactor

Siyuan Wang, [a] Quang Truong Le, [b] Yoshiteru Shishido,[c] Ismail Y. Kokculer, [c] Ken Yamazaki, [d] Gregory J. P. Perry, *[a] Adrian M. Nightingale *[b] and Hideki Yorimitsu *[c]

Received 4th August 2025
Accepted 22nd October 2025

DOI: 10.1039/d5sc05889a

rsc.li/chemical-science

The cleavage of C–S bonds in dibenzothiophene dioxides under reductive photoredox catalysed conditions is reported. The reactions afford sulfinates, which can be used in a variety of subsequent transformations for diversification. When using unsymmetrical dibenzothiophene substrates, reductive cleavage occurs preferentially at one C–S bond. Experimental and computational studies provide insight into this interesting selectivity. The process tolerates the presence of oil (dodecane), highlighting a possible application in the removal of dibenzothiophene impurities from crude oil. The reactivity of some substrates is highly dependent on reaction temperature, hence the development of a versatile and inexpensive 3D printed photoreactor that allows for the precise control of reaction temperature is also reported.

Sulfinate salts (RSO_2^-) are highly versatile compounds in synthesis.[1] They are routinely used to access a range of important functional groups such as sulfonamides, sulfones and sulfonyl fluorides, with applications in various fields, for example biology and medicine.[2] They can also be used in a variety of valuable cross-coupling reactions by extrusion of SO_2 to access important C–C and C–heteroatom bond linkages.[1]

Desulfonylation *via* reductive C–S bond cleavage of sulfones is highly useful in organic synthesis but generally requires strongly reducing metals.[3] Milder photocatalytic methods for C–S bond cleavage are known, but these routes often require activated substrates, for example sulfones containing heteroaromatic (azoles, pyridines *etc.*), alkenyl/alkynyl, polyfluoroalkyl, cyano or keto groups (Scheme 1A).[4]

Dibenzothiophene dioxides **1** are a class of relatively unactivated sulfones that can be easily accessed through routine oxidation of dibenzothiophenes. Recent investigations into the deconstruction of dibenzothiophene dioxides has resulted in a variety of useful C–S bond cleaving transformations that have found applications in synthesis and neighbouring fields.[5,6] Investigating the reactivity of dibenzothiophene dioxides may also deliver benefits in oxidative desulfurization for removing dibenzothiophene impurities from petroleum.[7]

Methods for the reductive cleavage of dibenzothiophene dioxides **1** are limited, especially from a synthetic perspective.

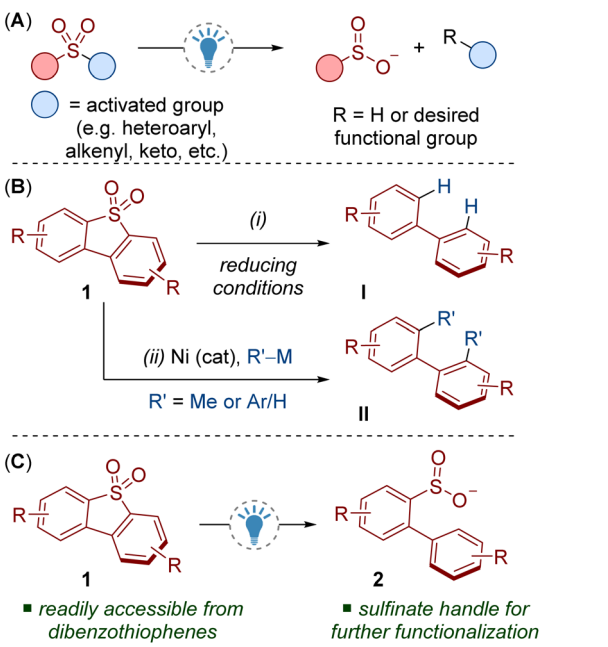

Scheme 1 (A) Photocatalytic cleavage of activated sulfones. (B) Reductive cleavage of dibenzothiophene dioxides. (C) This work: photoredox catalysed reductive cleavage of dibenzothiophene dioxides.

[a]*School of Chemistry and Chemical Engineering, University of Southampton, Southampton, SO17 1BJ, UK. E-mail: gregory.perry@soton.ac.uk*

[b]*Mechanical Engineering, Faculty of Engineering and Physical Sciences, University of Southampton, Southampton, SO17 1BJ, UK. E-mail: A.Nightingale@soton.ac.uk*

[c]*Department of Chemistry, Graduate School of Science, Kyoto University, Sakyo-ku, Kyoto, 606-8502, Japan. E-mail: yori@kuchem.kyoto-u.ac.jp*

[d]*Division of Applied Chemistry, Okayama University, Tsushimanaka, Okayama 700-8530, Japan*

For example, many methods lead to unfunctionalized biaryls **I** and require relatively forcing conditions (Scheme 1B, i).[8] More attractive cross-coupling methods have been demonstrated, but they suffer from low yields, product mixtures and/or poor generality (Scheme 1B, ii).[9] Both strategies also lead to the complete removal of the sulfur functionality. A complementary cleavage process that retains the sulfur moiety would deliver products with a synthetic handle for accessing various modes of reactivity and valuable functional groups.

Here we report a photocatalytic reductive C–S bond cleavage of dibenzothiophene dioxides **1** (Scheme 1C). The reaction produces sulfinates **2** which can be used as a platform for diversification, for example *via* fluorination, alkylation and cross-coupling reactions. Computational and experimental results provide insight into this unique mode of reactivity. To aid these studies, we also introduce a 3D printed photoreactor that will prove useful to others in need of precise temperature control for photochemical reactions.

Our previous work on sulfonamide functionalization provided a photoredox catalysed reduction of sulfonyl pyrroles.[10] With these conditions, our initial results were encouraging, showing that sulfinate **2a** (analysed as the corresponding sulfonyl fluoride **3a**) was formed in 38% yield from dibenzothiophene dioxide **1a** (Table 1, Entry 1). Interestingly, the sulfur functionality was retained under our conditions, providing a complementary approach to previous reductions in which the sulfone **1** is either reduced to the dibenzothiophene[11] or the SO_2 unit is lost completely (*c.f.* Scheme 1B),[8,9] and opens the possibility for further derivatization (*vide infra*, Scheme 5A). Further optimisation revealed that the removal of water and addition of formic acid had a beneficial effect on the reaction yield (Entry 2). Optimized conditions were achieved by switching the photoredox catalyst from **Ir1** to the more strongly reducing **Ir2** (Entry 3, **Ir1**: E_{red} [Ir^{III}/Ir^{II}] = −1.51 V *vs.* SCE in MeCN; **Ir2**: E_{red} [Ir^{III}/Ir^{II}] = −2.19 V *vs.* SCE in MeCN).[12] Finally, the reaction did not proceed in the absence of the light source or the photoredox catalyst.[13]

With a mild and efficient process in hand, we began to explore the scope of the reaction but found some substrates gave significantly lower yields. For example, 2,8-dimethyldibenzothiophene dioxide **1b** gave only 18% yield of product **3b** under the standard reaction conditions (Entry 4). We considered two possibilities for this decrease in reactivity: susceptibility towards reduction and solubility. Firstly, substrate **1b** may be less reactive as it is harder to reduce. This was reflected in the measured cathodic peak potentials (**1a**: E_{pc} = −1.7 V *vs.* SCE in MeCN, **1b**: E_{pc} = −2.2 V *vs.* SCE in MeCN).[13] A more strongly reducing photodeox catalyst, 10-phenylphenothiazine (PTH), showed an improvement in reactivity, but the yield was still unsatisfactory (Entry 5).[14] Secondly, substrate **1b** is relatively insoluble. For example, whereas ~18 mg mL^{-1} of **1a** was soluble in MeCN, only ~2 mg mL^{-1} of **1b** was soluble in MeCN.[13] In this regard, diluting the reaction mixture to 0.125 M showed a small improvement in yield (Entry 6). More polar solvents (DMF and DMSO) did not improve reactivity.[13] Ultimately, to better improve the solubility of the substrate and the overall reactivity of the system, we opted to increase the

Table 1 Optimisation of the photoredox catalysed reductive cleavage of dibenzothiophene dioxides[a]

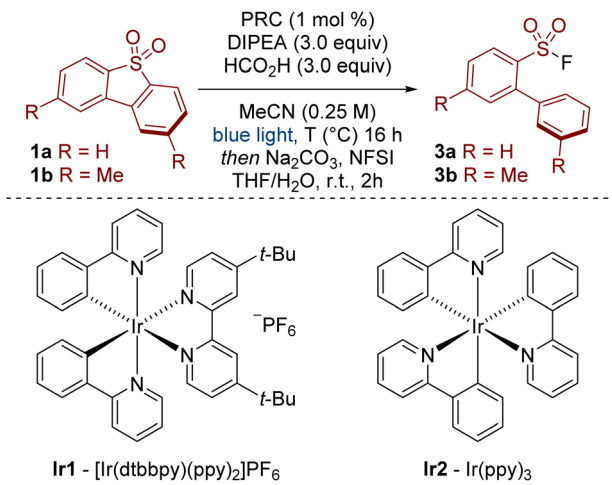

Ir1 - $[Ir(dtbbpy)(ppy)_2]PF_6$ **Ir2** - $Ir(ppy)_3$

Entry	R	PRC	T (°C)	**3a**/**3b** [b] (%)
1[c]	H	**Ir1**	25	38
2[d]	H	**Ir1**	25	44
3	H	**Ir2**	25	95 (93)[e]
4	Me	**Ir2**	25	18
5	Me	**PTH** [f]	25	36
6[g]	Me	**Ir2**	25	32
7	Me	**Ir2**	50	85 (82)[e]

[a] Reaction conditions: **1** (0.5 mmol), photoredox catalyst (PRC, 1 mol%), DIPEA (3.0 equiv.), HCO_2H (3.0 equiv.), MeCN (0.25 M), light = Kessil PR160L 440 nm, T = 25 °C or 50 °C, 16 h. Remove volatiles then Na_2CO_3 (1.5 equiv.), *N*-fluorobenzenesulfonimide (NFSI, 2.0 equiv.), THF/H_2O (9 : 1, 0.25 M). [b] ^1H NMR yields using $CHCl_2CHCl_2$ as an internal standard. [c] DIPEA = 4.0 equiv., HCO_2H = 0 equiv., solvent = MeCN/H_2O (6 : 1, 0.25 M). [d] DIPEA = 4.0 equiv., HCO_2H = 4.0 equiv. [e] Yield in parenthesis is of isolated material. [f] 10-Phenylphenothiazine (PTH, 5 mol%), light = Kessil PR160L 390 nm. [g] MeCN (0.125 M).

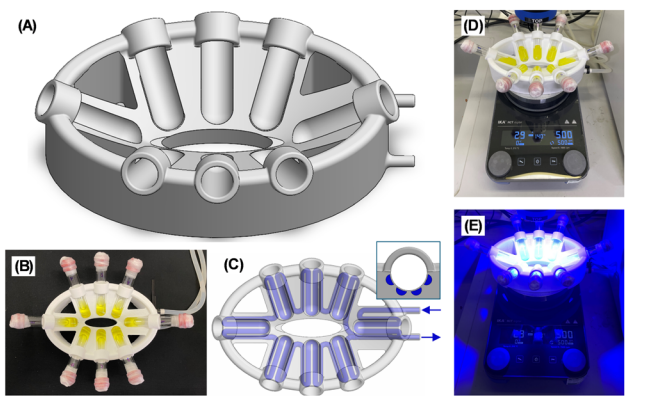

Fig. 1 (A) CAD image of the 3D printed photoreactor. (B) 3D Printed photoreactor with reaction vials. (C) CAD image of the 3D printed photoreactor demonstrating the recirculating fluid. (C, inset) cross section showing the position of the recirculating fluid channels relative to a vial (D) reaction set up. (E) Reaction set up under irradiation.

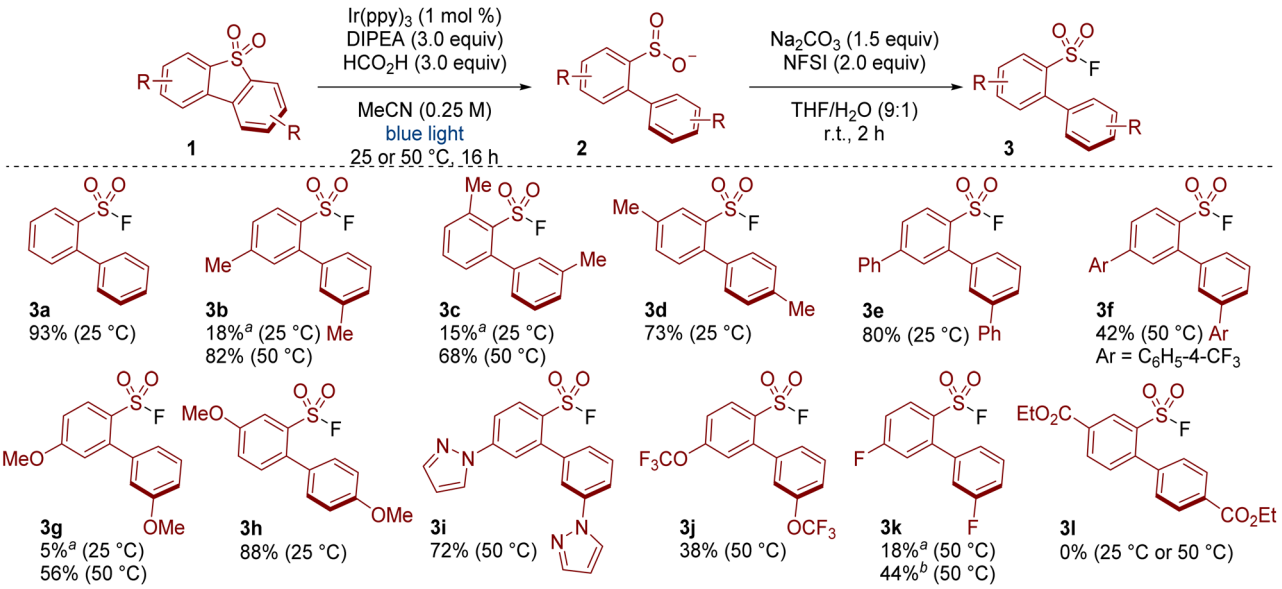

Scheme 2 Scope of the photoredox catalysed cleavage of symmetrical dibenzothiophene dioxides. [a] ^{1}H NMR yields using $CHCl_2CHCl_2$ as an internal standard. [b] $[Ir(dtbbpy)(ppy)_2]PF_6$ was used instead of $Ir(ppy)_3$.

temperature to 50 °C, which, gratifyingly, provided the product in high yield (Entry 7).

Although increasing the temperature of a reaction is usually a simple task, this proves challenging under photochemical conditions due to a lack of suitable equipment. For example, when first conducting the photoredox reactions with **1b** at 50 °C we had to part submerge the vials in a water bath, which was inconvenient, hazardous and impractical. Others have also been forced to use elaborate experimental setups when performing photochemical reactions at elevated or reduced temperatures.[15] Previously reported photoreactors were found to be unsuitable as they either do not allow for accurate temperature control and/or were prohibitively expensive bespoke models.[16] We therefore designed our own low-cost photoreactors that conveniently enable photochemical reactions at a range of temperatures (Fig. 1A).[17] The importance of temperature control in photochemical reactions has recently been highlighted by Cañellas and co-workers.[16j] Our photoreactors are 3D printed in polycarbonate using standard fused filament printers, making them low cost and easily accessible. The photoreactor can hold up to 8 vials (Fig. 1B), is designed to sit on a standard laboratory stirrer plate (Fig. 1D) and is oval shaped to match the illumination area for commonly used PR160L Kessil Lamps (ensuring each vial receives equal light intensity, Fig. 1E). Temperature-control is achieved by connection to a refrigerated/heating circulator. Liquid from the circulator is flowed through channels in the photoreactor body (Fig. 1C) located immediately behind each vial (Fig. 1C inset) allowing heat exchange with the vials without affecting the light path. Here we used water as the recirculating liquid to set the temperature at 25 or 50 °C, however we found temperatures between 10–80 °C were achievable. We envisage that the temperature range could be further extended using other recirculating liquids and reactor materials.

With conditions and set-up optimised, we then tested the method on a range of substrates. Screening was made easier with our 3D printed photoreactor as we were able to simply switch between temperatures when required. For example, products **3a**, **3d**, **3e** and **3h** formed in appreciable yields at 25 °C, whereas **3b**, **3c** and **3g** required heating. Substituents at various positions around the dibenzothiophene dioxide were tolerated (*e.g.* see **3b**, **3c**, **3d**). Products bearing phenyl (**3e**, **3f**) and methoxy substituents (**3g**, **3h**) also formed in respectable yield. Some heteroaromatics were also tolerated, as demonstrated in the formation of the pyrazole-containing product **3i.** Reactivity was also observed with trifluoromethoxy and fluoro

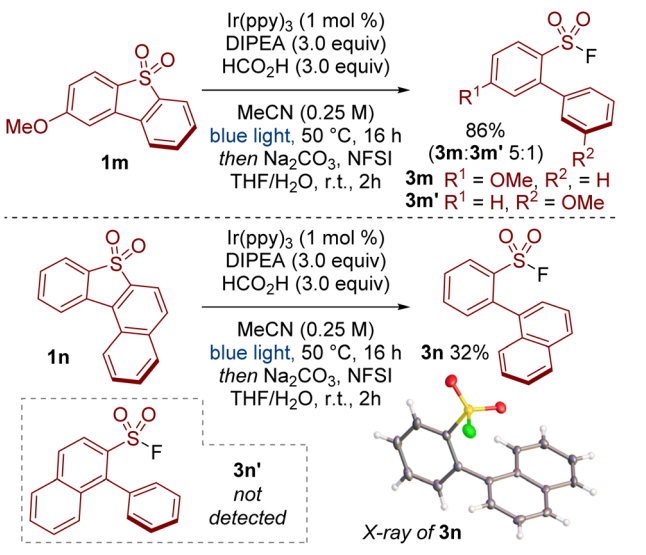

Scheme 3 Scope of the photoredox catalysed cleavage of unsymmetrical dibenzothiophene dioxides.

substituents (**3j** and **3k**). A substrate bearing an ester substituent gave none of the desired product **3l**. The poor reactivity in this case may be due to the low solubility of the compound (<1 mg mL^{-1} in MeCN).[13] Other unsuccessful substrates and details on the outcome of these reactions are provided in the SI (Table S4).

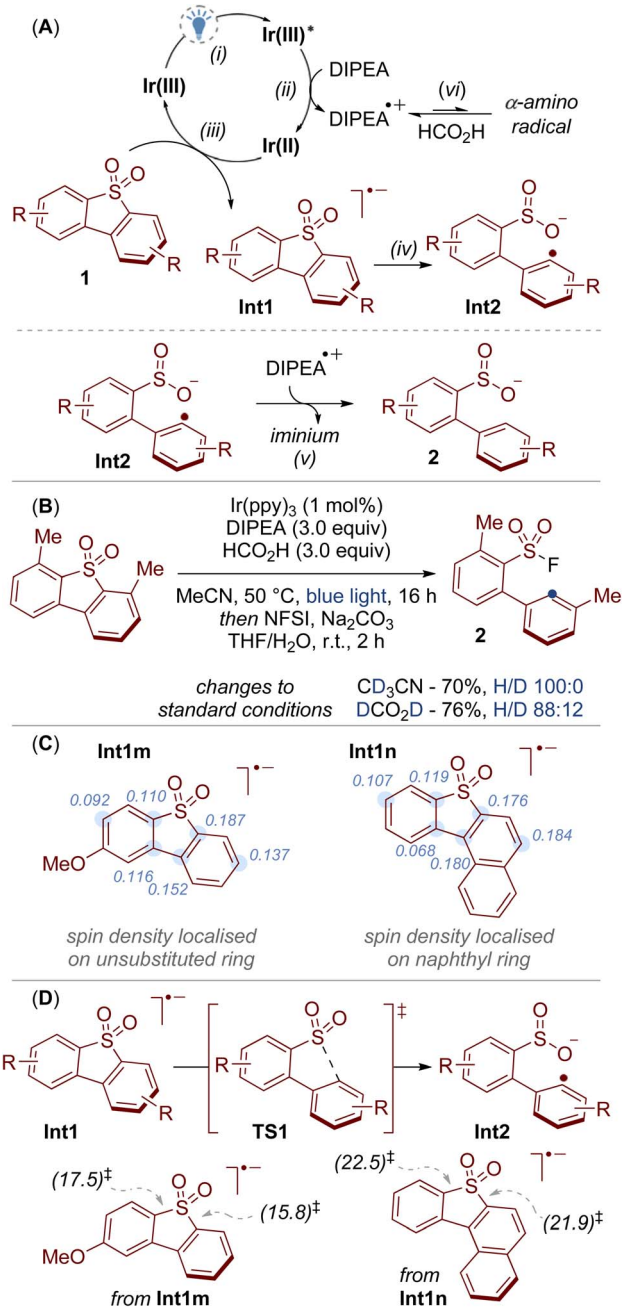

Scheme 4 Mechanistic studies. (A) Proposed mechanism for the photoredox catalysed reductive C–S bond cleavage. (B) Deuterium labelling experiments. (C) NBO spin density analysis of radical anion intermediates. Major spin density values are shown. (D) Potential energy diagram for the C–S bond cleavage of unsymmetrical dibenzothiophene dioxides computed at the SMD(MeCN)/M06-2X/6-311++G(d,p)//SMD(MeCN)/B3LYP-D3/6-31+G(d) level of theory. Activation energy barriers ($\Delta G^{\ddagger}$ [kcal mol^{-1}]) are provided in the insert.

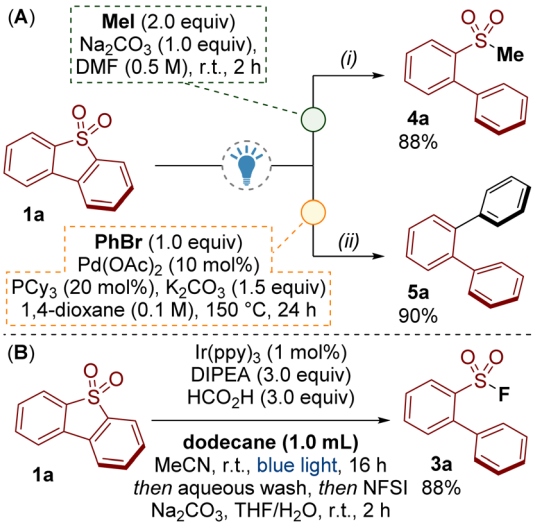

Scheme 5 (A) Derivatisations of the sulfinate products. (B) Tolerance of the reaction towards dodecane.

When testing unsymmetrical dibenzothiophene dioxides, we observed some impressive selectivity (Scheme 3). For example, substrate **1m** was cleaved to give product **3m** preferentially over isomer **3m′**. Similarly, reductive cleavage of **1n** provided **3n** exclusively; the other isomer **3n′** was not observed. The structure of **3n** was unequivocally determined by X-ray crystallography.[18]

A simplified mechanism for this reaction is provided in Scheme 4A. We propose a reductive quenching cycle in which a highly reducing iridium species **Ir(II)** is generated from exposure of the excited state catalyst **Ir(III)*** to DIPEA (step i, and ii).[19] This causes the reduction of the dibenzothiophene dioxide **1** to give the radical anion **Int1** (step iii), which subsequently undergoes spontaneous C–S bond cleavage to the radical species **Int2** (step iv).[20] We then tentatively propose that hydrogen atom transfer between **Int2** and the radical cation $DIPEA^{\bullet+}$ provides the sulfinate salt **2** (step v).[21] Under the standard conditions, the sulfinate salt **2** is transformed into the sulfonyl fluoride **3** through subsequent treatment with NFSI.

To provide support for this mechanism we first conducted a series of deuterium labelling experiments (Scheme 4B). Under otherwise standard conditions, deuterium incorporation was not observed when deuterated solvent (CD_3CN) was used, and only a small amount (12%) was incorporated when using deuterated formic acid (DCO_2D). We therefore suggest that DIPEA is the main hydrogen atom source for this reaction, which we tentatively propose is incorporated through hydrogen atom transfer between **Int2** and the radical cation of the amine (Scheme 4A, step v).[21] One possibility for the role of formic acid is that it impedes deprotonation of the radical cation $DIPEA^{\bullet+}$, thereby lessening the formation of α-amino radicals that may otherwise lead to unproductive side reactions (Scheme 4A, step vi).[22]

Computational studies provided insight into the interesting selectivity we observed with unsymmetrical dibenzothiophene dioxides (*c.f.* Scheme 3). When modelling the radical anion

intermediates **Int1m** and **Int1n** it was found that the non-bonding orbital (NBO) spin density was localised on the aromatic ring that underwent C–S bond cleavage (Scheme 4C). In addition, DFT calculations suggested that the energy barriers *via* C–S bond cleavage transition state **TS1** were lower in energy for the pathways that led to products **3m** and **3n** in comparison to the pathways towards isomers **3m′** and **3n′** (Scheme 4D). For example, cleavage of the C–S bond that led to the formation of **3m** was calculated to have an energy barrier of 15.8 kcal mol^{-1}, whereas the pathway to the minor isomer **3m′** required a higher energy input of 17.5 kcal mol^{-1}. Thus, calculation of the spin density of the radical anion intermediates **Int1** provides a tool for predicting the site selectivity for C–S bond cleavage.

An advantage of our photoredox catalysed methodology over related reductive processes (*c.f.* Scheme 1B) is that the sulfur moiety remains present as a sulfinate at the end of the reaction. In addition to fluorination (Scheme 2), we have shown the utility of the sulfinate products by accessing sulfones **4a** and performing a palladium catalysed desulfinylative cross-coupling to give *ortho*-terphenyl **5a** (Scheme 5A).[23]

Finally, oxidative desulfurization is a process for removing dibenzothiophene impurities from petroleum *via* oxidation to the dibenzothiophene dioxide and subsequent extraction. Significant achievements have been made in this area though several drawbacks remain, including efficient separation of the dibenzothiophene dioxide from the crude oil.[7] Scheme 5B shows that our method was tolerant of an excess of dodecane oil. In this process, dibenzothiophene **1a** was converted to the sulfinate salt **2a**, which was easily removed from dodecane by extraction with water. The fluorination step to give **3a** was performed to demonstrate the recovery of the sulfinate. Though primitive, transforming dibenzothiophene dioxides **1** into water soluble/oil-immiscible sulfinate salts **2** presents an alternative concept for oxidative desulfurization.

Conclusions

We have developed a photoredox catalysed reductive cleavage of C–S bonds in dibenzothiophene dioxides **1**. The sulfinates **2** that were accessed through this route were transformed into a variety of products, such as sulfonyl fluorides **3**, sulfones **4** and biaryls **5**. Experimental and computational studies provided insight into the reaction mechanism and the impressive selectivity observed with unsymmetrical substrates. In addition, we designed and developed a 3D printed photoreactor that allowed the temperature of the process to be accurately controlled and offers a practical, accessible and low-cost set-up for performing photochemical reactions at reduced or elevated temperatures.

Author contributions

GJPP and HY conceptualised the chemical reaction. SW, YS, IYK and GJPP performed the chemical reactions. GJPP and AMN conceptualised the 3D printed photoreactor. TL and AMN developed the 3D printed photoreactor. KY performed DFT calculations. SW and GJPP prepared the SI for the chemical reactions. TL, AMN and GJPP prepared the SI for the 3D printed photoreactor. GJPP wrote the original draft of the manuscript. GJPP, AMN and HY reviewed and edited the manuscript and SI. GJPP and HY obtained funding for the project.

Conflicts of interest

There are no conflicts of interest to declare.

Data availability

CCDC 2427585 (**3a**) and 2408586 (**3n**) contain the supplementary crystallographic data for this paper.[18a,b]

The data supporting this article have been included as part of the supplementary information (SI). Supplementary information is available. See DOI: **https://doi.org/10.1039/d5sc05889a**.

Acknowledgements

This work was supported by a Royal Society Research Grant (RGS\R2\242219), an RSC Researcher Collaborations Grant (C24-8914031093), an RSC Research Fund (R24-6800702932) a Daiwa Foundation Small Grant (14880/15735) and a JSPS Postdoctoral Fellowship for Research in Japan (KAKENHI Grant No. JP21F21039). This work was partly supported by a JSPS KAKENHI Grant in Transformative Research Areas (A) (JP24H02208), an Integrated Science of Synthesis by Chemical Structure Reprogramming Grant (SReP) (JP24A202) and a JST CREST Grant in Innovative Reactions (JPMJCR19R4). The computational analysis was performed using the Research Center for Computational Science, Okazaki, Japan (Project: 25-IMS-C248). We thank Georgios Retsidis, Professor Richard C. D. Brown and Professor Peter R. Birkin for guidance with the cyclic voltammetry measurements. We thank Dr Julie Herniman, Dr Neil J. Wells and Dr Mark E. Light for leading the mass spectrometry, NMR spectroscopy and X-ray diffraction facilities within the University of Southampton.

Notes and references

1 (*a*) E. J. Emmett and M. C. Willis, *Asian J. Org. Chem.*, 2015, **4**, 602–611; (*b*) D. Kaiser, I. Klose, R. Oost, J. Neuhaus and N. Maulide, *Chem. Rev.*, 2019, **119**, 8701–8780; (*c*) J. M. Smith, J. A. Dixon, J. N. deGruyter and P. S. Baran, *J. Med. Chem.*, 2019, **62**, 2256–2264; (*d*) S. Liang, K. Hofman, M. Friedrich and G. Manolikakes, *Eur. J. Org Chem.*, 2020, **2020**, 4664–4676; (*e*) G. J. P. Perry and H. Yorimitsu, *ACS Sustainable Chem. Eng.*, 2022, **10**, 2569–2586; (*f*) Z. Lu, M. Shang and H. Lu, *Synthesis*, 2022, **54**, 1231–1249; (*g*) T. S.-B. Lou and M. C. Willis, *Nat. Rev. Chem.*, 2022, **6**, 146–162.

2 (*a*) J. Dong, L. Krasnova, M. G. Finn and K. B. Sharpless, *Angew. Chem., Int. Ed.*, 2014, **53**, 9430–9448; (*b*) P. Devendar and G.-F. Yang, *Top. Curr. Chem.*, 2017, **375**, 82; (*c*) K. A. Scott and J. T. Njardarson, *Top. Curr. Chem.*, 2018, **376**, 5.

3 (*a*) P. Kocienski, *Phosphorus Sulfur Relat. Elem.*, 1985, **24**, 97–127; (*b*) R. Dumeunier and I. E. Markó, in *Modern Carbonyl Olefination*, ed. T. Takeda, Wiley, 1st edn, 2003, pp. 104–150; (*c*) D. A. Alonso, C. Nájera, in *Organic Reactions*, Wiley, 2009, pp. 367–656; (*d*) M. Szostak, M. Spain and D. J. Procter, *Chem. Soc. Rev.*, 2013, **42**, 9155.

4 (*a*) M. Nambo, Y. Maekawa and C. M. Crudden, *ACS Catal.*, 2022, **12**, 3013–3032; (*b*) J. Corpas, S.-H. Kim-Lee, P. Mauleón, R. G. Arrayás and J. C. Carretero, *Chem. Soc. Rev.*, 2022, **51**, 6774–6823.

5 (*a*) T. Aida, T. G. Squares and C. G. Venier, *Tetrahedron Lett.*, 1983, **24**, 3543–3546; (*b*) M. Bhanuchandra, K. Murakami, D. Vasu, H. Yorimitsu and A. Osuka, *Angew. Chem., Int. Ed.*, 2015, **54**, 10234–10238; (*c*) M. Bhanuchandra, H. Yorimitsu and A. Osuka, *Org. Lett.*, 2016, **18**, 384–387; (*d*) S. Adak and T. P. Begley, *J. Am. Chem. Soc.*, 2016, **138**, 6424–6426; (*e*) K. Nogi and H. Yorimitsu, *Chem. Commun.*, 2017, **53**, 4055–4065; (*f*) M. Onoda, Y. Koyanagi, H. Saito, M. Bhanuchandra, Y. Matano and H. Yorimitsu, *Asian J. Org. Chem.*, 2017, **6**, 257–261; (*g*) S. Mylavarapu, M. Yadav and M. Bhanuchandra, *Org. Biomol. Chem.*, 2018, **16**, 7815–7819; (*h*) A. Kaga, K. Nogi and H. Yorimitsu, *Chem.–Eur. J.*, 2019, **25**, 14780–14784; (*i*) T. Furukawa, T. Yanagi, A. Kaga, H. Saito and H. Yorimitsu, *Helv. Chim. Acta*, 2021, **104**, e202100195; (*j*) M. Yadav, R. Singh Jat, S. Kumari, P. Vijaya Babu, P. Roy and M. Bhanuchandra, *Tetrahedron Lett.*, 2023, **119**, 154430; (*k*) H. Yorimitsu and J. Synth, *J. Synth. Org. Chem., Jpn.*, 2024, **82**, 420–432; (*l*) H. Yorimitsu, *Acc. Chem. Res.*, 2025, **58**, 1323–1334.

6 (*a*) V. Govindan, K.-C. Yang, Y.-S. Fu and C.-G. Wu, *New J. Chem.*, 2018, **42**, 7332–7339; (*b*) G. Xia, C. Qu, Y. Zhu, J. Ye, K. Ye, Z. Zhang and Y. Wang, *Angew. Chem., Int. Ed.*, 2021, **60**, 9598–9603; (*c*) T. Yanagi, T. Tanaka and H. Yorimitsu, *Chem. Sci.*, 2021, **12**, 2784–2793; (*d*) T. D. Weinhold, N. A. Reece, K. Ribeiro, M. Lopez Ocasio, N. Watson, K. Hanson and A. R. Longstreet, *J. Org. Chem.*, 2022, **87**, 16928–16936; (*e*) X. Deng, S. Liu, Y. Sun, D. Zhong, D. Jia, X. Yang, B. Su, Y. Sun, G. Zhou, B. Jiao and Z. Wu, *Dyes Pigm.*, 2023, **209**, 110885; (*f*) J. Cai, G. Zeng, K. Jiang, H. Luo and B. Yin, *Org. Lett.*, 2024, **26**, 327–331; (*g*) C. Lu, J. Y. Choi, B. Check, X. Fang, S. Spotts, D. Nuñez and J. Park, *J. Am. Chem. Soc.*, 2024, **146**, 26313–26319.

7 (*a*) A. Rajendran, T. Cui, H. Fan, Z. Yang, J. Feng and W. Li, *J. Mater. Chem. A*, 2020, **8**, 2246–2285; (*b*) Q. Shi and J. Wu, *Energy Fuels*, 2021, **35**, 14445–14461; (*c*) Z. Sun and R. Wang, *Fuel*, 2025, **402**, 136031.

8 (*a*) W. S. Jenks, L. M. Taylor, Y. Guo and Z. Wan, *Tetrahedron Lett.*, 1994, **35**, 7155–7158; (*b*) C. Kuehm-Caubère, A. Guilmart, S. Adach-Becker, Y. Fort and P. Caubère, *Tetrahedron Lett.*, 1998, **39**, 8987–8990; (*c*) S. Becker, Y. Fort and P. Caubere, *J. Org. Chem.*, 2002, **55**, 6194–6198; (*d*) Z. Yu and J. G. Verkade, *Phosphorus, Sulfur Silicon Relat. Elem.*, 2006, **133**, 79–82; (*e*) D. P. Morales, A. S. Taylor and S. C. Farmer, *Molecules*, 2010, **15**, 1265–1269; (*f*) M. Pittalis, U. Azzena and L. Pisano, *Tetrahedron*, 2013, **69**, 207–211; (*g*) M. Shakirullah, W. Ahmad, I. Ahmad, M. Ishaq and M. I. Khan, *RSC Adv.*, 2013, **3**, 10673; (*h*) A. V. Vutolkina, A. V. Akopyan, A. P. Glotov, M. S. Kotelev, A. L. Maksimov and E. A. Karakhanov, *Russ. J. Appl. Chem.*, 2018, **91**, 981–989; (*i*) F. Chang and A. Fedorov, *Chem.–Eur. J.*, 2022, **28**, e202201574; (*j*) H. Liu, Y. Wang, F. Zhang, C. Xu, X. Liao, Y. Jiang and S. Lu, *New J. Chem.*, 2022, **46**, 3409–3416.

9 (*a*) A. Oviedo, J. Torres-Nieto, A. Arévalo and J. J. García, *J. Mol. Catal. A: Chem.*, 2008, **293**, 65–71; (*b*) A. Oviedo, A. Arévalo, M. Flores-Alamo and J. J. García, *Organometallics*, 2012, **31**, 4039–4045; (*c*) R. Gutiérrez-Ordaz and J. J. García, *Polyhedron*, 2018, **154**, 373–381.

10 (*a*) T. Ozaki, H. Yorimitsu and G. J. P. Perry, *Chem.–Eur. J.*, 2021, **27**, 15387–15391; (*b*) T. Ozaki, H. Yorimitsu and G. J. P. Perry, *Tetrahedron*, 2022, **117–118**, 132830.

11 (*a*) H. Sirringhaus, R. H. Friend, C. Wang, J. Leuninger and K. Müllen, *J. Mater. Chem.*, 1999, **9**, 2095–2101; (*b*) K. Kawabata, M. Takeguchi and H. Goto, *Macromolecules*, 2013, **46**, 2078–2091.

12 C. K. Prier, D. A. Rankic and D. W. C. MacMillan, *Chem. Rev.*, 2013, **113**, 5322–5363.

13 See the SI for further details.

14 (*a*) E. H. Discekici, N. J. Treat, S. O. Poelma, K. M. Mattson, Z. M. Hudson, Y. Luo, C. J. Hawker and J. R. De Alaniz, *Chem. Commun.*, 2015, **51**, 11705–11708; (*b*) M. H. Aukland, M. Šiaučiulis, A. West, G. J. P. Perry and D. J. Procter, *Nat. Catal.*, 2020, **3**, 163–169.

15 For example, see the supporting information in: (*a*) J. J. Douglas, K. P. Cole and C. R. J. Stephenson, *J. Org. Chem.*, 2014, **79**, 11631–11643; (see Fig. S5 and accompanying text); (*b*) A. Ruffoni, C. Hampton, M. Simonetti and D. Leonori, *Nature*, 2022, **610**, 81–86.

16 (*a*) P. P. Lampkin, B. J. Thompson and S. H. Gellman, *Org. Lett.*, 2021, **23**, 5277–5281; (*b*) F. Schiel, C. Peinsipp, S. Kornigg and D. Böse, *ChemPhotoChem*, 2021, **5**, 431–437; (*c*) O. Wallner, K. Mamonov, F. Ortis, D. Michel and M. Michel, *Chem.: Methods*, 2021, **1**, 240–244; (*d*) T. D. Svejstrup, A. Chatterjee, D. Schekin, T. Wagner, J. Zach, M. J. Johansson, G. Bergonzini and B. König, *ChemPhotoChem*, 2021, **5**, 808–814; (*e*) E. G. Gordeev, K. S. Erokhin, A. D. Kobelev, J. V. Burykina, P. V. Novikov and V. P. Ananikov, *Sci. Rep.*, 2022, **12**, 3780; (*f*) M. R. Penny and S. T. Hilton, *J. Flow Chem.*, 2023, **13**, 435–442; (*g*) T. Aubineau, J. Laurent, L. Olanier and A. Guérinot, *Chem.: Methods*, 2023, **3**, e202300002; (*h*) J. W. Rackl, A. F. Müller, C. Bärtschi and H. Wennemers, *Helv. Chim. Acta*, 2024, **107**, e202400154; (*i*) J. Zhang, E. Selmi-Higashi, S. Zhang, A. Jean, S. T. Hilton, X. C. Cambeiro and S. Arseniyadis, *Org. Lett.*, 2024, **26**, 2877–2882; (*j*) B. Pijper, L. M. Saavedra, M. Lanzi, M. Alonso, A. Fontana, M. Serrano, J. E. Gómez, A. W. Kleij, J. Alcázar and S. Cañellas, *JACS Au*, 2024, **4**, 2585–2595.

17 Further information on the photoreactor set-up and the printing of the photoreactor can be found in the SI along with the design (.stl) files.

18 (*a*) CCDC 2427585: Experimental Crystal Structure Determination, 2025, DOI: **10.5517/ccdc.csd.cc2mh36g**; (*b*)

CCDC 2408586: Experimental Crystal Structure Determination, 2025, DOI: 10.5517/ccdc.csd.cc2lvbb4.

19 R. N. Motz, A. C. Sun, D. Lehnherr and S. Ruccolo, *ACS Org. Inorg. Au*, 2023, **3**, 266–273.

20 Upon formation of **Int2**/**2**, further C–S bond cleavage is not possible due to the stability of the sulfinate towards reduction.

21 J. M. R. Narayanam, J. W. Tucker and C. R. J. Stephenson, *J. Am. Chem. Soc.*, 2009, **131**, 8756–8757.

22 (*a*) J. P. Dinnocenzo and T. E. Banach, *J. Am. Chem. Soc.*, 1989, **111**, 8646–8653; (*b*) X. Zhang, S.-R. Yeh, S. Hong, M. Freccero, A. Albini, D. E. Falvey and P. S. Mariano, *J. Am. Chem. Soc.*, 1994, **116**, 4211–4220; (*c*) K. Nakajima, Y. Miyake and Y. Nishibayashi, *Acc. Chem. Res.*, 2016, **49**, 1946–1956; (*d*) M. L. Czyz, M. S. Taylor, T. H. Horngren and A. Polyzos, *ACS Catal.*, 2021, **11**, 5472–5480; (*e*) M. Lepori, S. Schmid and J. P. Barham, *Beilstein J. Org. Chem.*, 2023, **19**, 1055–1145.

23 T. Markovic, B. N. Rocke, D. C. Blakemore, V. Mascitti and M. C. Willis, *Chem. Sci.*, 2017, **8**, 4437–4442.